THERMOELECTRIC SIZE EFFECT IN AN ALTERNATING MAGNETIC FIELD AND ITS USE FOR THE STUDY OF PHASE TRANSITIONS

B. V. Avdeev, N. I. Varich, Yu. P. Krasheninin, M. A. Markman, and E. L. Nagaev
Submitted 22 January 1970
ZhETF Pis. Red. 11, No. 5, 241 - 244 (5 March 1970)

As is well known, an electric field perpendicular both to the temperature gradient and to the magnetic field is produced in an unevenly heated conductor placed in a magnetic field perpendicular to the temperature gradient (the Nernst effect). If the magnetic field is periodic, the phase of the transverse Nernst thermal emf coincides with the phase of the magnetic field. It will be shown below that in an alternating magnetic field, besides the usual Nernst effect, there is produced one more component of the transverse thermal emf, shifted in phase relative to the former by $\pi/2$. This component cannot be described phenomenologically by introducing the imaginary part of the Nernst coefficient, since it depends on the geometry of the sample, particularly on its dimensions. It turns out to be possible to separate experimentally these two components, so that one can speak of a second transverse thermomagnetic effect, which is realized in alternating magnetic fields.

The corresponding signal is proportional to the temperature derivative of the resistance ρ. This effect is very convenient for the investigation of singularities of $d\rho/dT$ near the critical point, since it makes it possible to avoid the errors arising in the numerical differentiation of the $\rho(T)$ curve. We used it to study $d\rho/dT$ in $MnTe_2$ crystals, where it revealed a sharp difference in the critical behavior of ρ as a function of the carrier density.

To obtain an expression for the "second" transverse thermal emf, it is assumed that the sample is a plate of infinite length in the direction of the X axis and is bounded by the planes $\pm L$ in the Y direction. The temperature gradient is directed along the X axis, and the magnetic field $\vec{B}(t) = \vec{B}_0 \exp(i\omega t)$ along the Z axis. The amplitude of the alternating electric field $\vec{E}$, which has the same time dependence, can be represented as the sum of the solenoidal part $\vec{E}_s$ and a potential part $\nabla\varphi$. The former is determined from the solution of Maxwell's equation

$$E_s = \{ -\frac{i\omega}{c} B_z y, 0, 0 \} . \qquad (1)$$

The real part of $\nabla\varphi$ is the usual Nernst thermal emf. On the other hand, to determine $\mathrm{Im}\,\nabla\varphi \equiv \nabla\varphi''$ it is possible to use the continuity equation for the current, which in the linear approximation in $\vec{B}$ and ∇T reduces here to the equality

$$\sigma \Delta \phi'' = -\mathrm{Im} E_s \nabla\sigma = -\mathrm{Im} E_s \nabla T \frac{d\sigma}{dT} , \qquad (2)$$

where σ is the conductivity of the sample. Integration of (2) with allowance for (1) and for the boundary condition for the currents $j_y(\pm L) = 0$ yields the following expression for the sought potential difference

$$\phi''(L) - \phi''(-L) = \frac{\omega B_z}{c} \frac{1}{\sigma} \frac{d\sigma}{dT} (\nabla T)_x L^3. \qquad (3)$$

This effect was experimentally investigated with a setup for the measurement of the Nernst effect in an alternating magnetic field. The use of a phase detector based on a Hall pickup has made it possible to discriminate between the signal phases. The measurements were made at 50 Hz, in fields up to 1 kOe, at temperature gradients from 1 to 3 deg/cm. The sensitivity of the setup reaches 10^{-9} V.

We investigated single crystals of $MnTe_2$ produced by the hot pressing method. The measured samples were parallelepipeds measuring 20 x 5 x 3 mm. To decrease the lateral heat losses, the gradient was directed along the shortest side. Although such a geometry differs from that for which the calculation was performed, the qualitative laws remain valid also for this case. $MnTe_2$ crystals were chosen because at room temperatures they undergo a phase transition from the antiferromagnetic to the paramagnetic state. Figure 1 shows plots of $(1/\rho)d\rho/dT$ obtained by direct measurement with the setup, and Fig. 2 shows for comparison the experimental $\sigma(T)$ curves. Curves 1 and 2 correspond to samples with carrier densities on the order of 10^{18} and 10^{20} cm^{-3}, respectively.

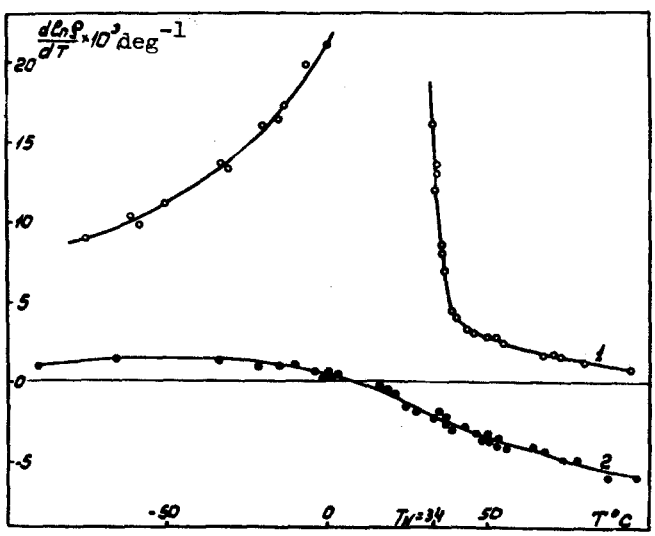

Fig. 1

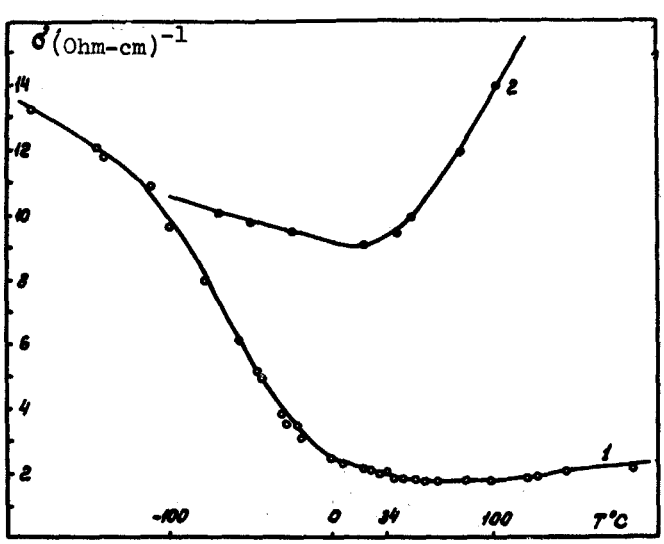

Fig. 2

A comparison of the experimentally observed potential difference with that calculated by formula (3), where the values of $(1/\sigma)d\sigma/dT$ were taken from Fig. 2, shows that both quantities are of the same order. The lack of exact agreement can be naturally attributed to the difference between the geometries of the real sample and the one for which the calculation was performed.

Attention is called to the strong difference in the behavior of the samples having different carrier densities (curves 1 and 2) near the critical point. In the former case $(1/\rho)d\rho/dT$ shows a clearly pronounced singularity at $T < T_N$ (T_N is the Neel temperature), where it is proportional

to $(T_N - T)^{-0.8}$, whereas at $T > T_N$ it is proportional to $(T - T_N)^{-0.5}$.

In the second case no singularities of $(1/\rho)d\rho/dT$ were observed at the critical point. The conductivity at the Neel point passes through a clearly pronounced minimum, i.e., $d\rho/dT$ reverses sign.

The difference in the behavior of the crystals near the critical point can be attributed to the fact that the concept of second-order phase transition becomes meaningless in strongly doped crystals [1] and, as is well known, the specific-heat singularity disappears. It is quite natural that the similar singularity of $d\rho/dT$ disappears. The fact that the resistance passes through a maximum near the "former critical point" can be attributed to the role played in strongly doped semiconductors by impurity scattering. Besides scattering due to the electric field of the defects, an important role may be played also by scattering due to the disturbance of the magnetic order by the impurity. As shown in [2], the radius of the region in which the magnetic order is perturbed by the defect tends to infinity as $T \to T_N$, since this mechanism of scattering becomes most significant near T_N.

The authors are grateful to L. D. Dudkin for great help in the work and for supplying the samples.

[1] M. A. Mikulinskii, Zh. Eksp. Teor. Fiz. 53, 1071 (1967) [Sov. Phys.-JETP 26, 637 (1968)].
[2] R. M. White and R. B. Woolsey, Phys. Lett. 27A, 428 (1968).

NEW METHOD FOR GENERATING A GIANT PULSE IN OPTICAL GENERATORS

A. L. Mikaelyan, V. F. Kuprishov, Yu. G. Turkov, Yu. V. Andreev, and A. A. Shcherbakova
Submitted 23 January 1970
ZhETF Pis. Red. 11, No. 5, 244 - 246 (5 March 1970)

In this paper we describe a new method of generating giant pulses in a ruby laser; this method does not call for additional modulating elements to be introduced into the resonator. Giant-pulse generagion is obtained in a definite class of resonators as a result of changes occurring in the active sample during the generation process. We first present the experimental results.

The construction of the generator in question was described in [1]. We used a ruby crystal with sapphire end pieces, of 7 mm diameter and 120 mm length (the total crystal length was 157 mm). The excitation was by a straight IFP-1200 flash lamp. The resonator consisted of a totally reflecting spherical mirror with curvature radius $R \approx 41$ cm and a plane-parallel quartz plate 6 mm thick. To eliminate self-excitation of the generator as the result of reflections from the end faces of the crystal, the axis of the latter was tilted approximately 1° to the resonator axis.

The generation regime of the described laser depends significantly on the resonator length L. At values of L corresponding to the region of resonator stability (i.e., smaller than the effective curvature radius of the spherical mirror ($R_{eff} = R + l(1 - 1/n)$, where n is the refractive index of ruby), the usual free generation takes place, accompanied by random pulsations of the radiation (spikes). When L is increased until the resonator becomes unstable, the character of the generation changes sharply, and giant pulses appear in addition to the free generation spikes. This is illustrated in Fig. 1a, which shows an oscillogram